Coarse-grained stochastic models for tropical convection and climate

Boualem Khouider[†], Andrew J. Majda[†‡§], and Markos A. Katsoulakis[¶]

[†]Courant Institute of Mathematical Sciences and [‡]Center for Atmosphere and Ocean Sciences, New York University, New York, NY 10012; and [¶]Department of Mathematics and Statistics, University of Massachusetts, Amherst, MA 01003

Contributed by Andrew J. Majda, August 4, 2003

Prototype coarse-grained stochastic parametrizations for the interaction with unresolved features of tropical convection are developed here. These coarse-grained stochastic parametrizations involve systematically derived birth/death processes with low computational overhead that allow for direct interaction of the coarse-grained dynamical variables with the smaller-scale unresolved fluctuations. It is established here for an idealized prototype climate scenario that, in suitable regimes, these coarse-grained stochastic parametrizations can significantly impact the climatology as well as strongly increase the wave fluctuations about an idealized climatology.

The current practical models for prediction of both weather and climate involve general circulation models (GCMs) where the physical equations for these extremely complex flows are discretized in space and time and the effects of unresolved processes are parametrized according to various recipes. With the current generation of supercomputers, the smallest possible mesh spacings are ≈50–100 km for short-term weather simulations and of order 200–300 km for short-term climate simulations. There are many important physical processes that are unresolved in such simulations such as the mesoscale sea-ice cover, the cloud cover in subtropical boundary layers, and deep convective clouds in the tropics. An appealing way to represent these unresolved features is through a suitable coarse-grained stochastic model that simultaneously retains crucial physical features of the interaction between the unresolved and resolved scales in a GCM. In recent work in two different contexts, the authors have developed both a systematic stochastic strategy (1) to parametrize key features of deep convection in the tropics involving suitable stochastic spin-flip models and also a systematic mathematical strategy to coarse-grain such microscopic stochastic models (2) to practical mesoscopic meshes in a computationally efficient manner while retaining crucial physical properties of the interaction. This last work (2) is general with potential applications in material sciences, sea-ice modeling, etc. Crucial new scientific issues involve the fashion in which a stochastic model effects the climate mean state and the strength and nature of fluctuations about the climate mean. The main topic of this article is to discuss development of a family of coarse-grained stochastic models for tropical deep convection by combining the systematic strategies from refs. 1 and 2 and to explore their effect on both the climate mean and fluctuations for an idealized prototype model parametrization in the simplest scenario for tropical climate involving the Walker circulation, the east–west climatological state that arises from local region of enhanced surface heat flux, mimicking the Indonesian marine continent.

The Microscopic Stochastic Model for Convective Inhibition (CIN)

In a typical GCM, the fluid dynamical and thermodynamical variables, denoted here by the generic vector $\vec{u}$, are regarded as known only over a discrete horizontal mesh with $\vec{u}_j = \vec{u}(j\Delta x, t)$ denoting these discrete values. Throughout the discussion in this article, one horizontal spatial dimension along the equator in the east–west direction is assumed for simplicity in notation and explanation. As mentioned above, the typical mesh spacing in a GCM is coarse with Δx ranging from 50 to 250 km depending on the time duration of the simulation. On the other hand, observationally, CIN is known to have significant fluctuations on a horizontal spatial scale on the order of 1 km, the microscopic scale here, with changes in CIN attributed to different mechanisms in the turbulent boundary layer such as gust fronts, gravity waves, and turbulent fluctuations in equivalent potential temperature (3). In ref. 1 it was proposed that all these different microscopic physical mechanisms and their interaction, which increase and decrease CIN, are too complex to model in detail in a coarse-mesh GCM parametrization and instead, as in statistical mechanics, should be modeled by a simple order parameter, σ_I, taking only two discrete values:

$$\begin{aligned}&\sigma_I = 1 \text{ at a site if convection is inhibited (a CIN site)}\\ &\sigma_I = 0 \text{ at a site if there is potential for deep convection}\\ &\quad\text{[a potential for deep convection (PAC) site].}\end{aligned} \qquad [1]$$

The value of CIN at a given coarse-mesh point is determined by the averaging of CIN over the microscopic states in the vicinity of the given mesh point, i.e.,

$$\bar{\sigma}_I(j\Delta x, t) = \frac{1}{\Delta x}\int_{(j-1/2)\Delta x}^{(j+1/2)\Delta x} \sigma_I(x, t)dx. \qquad [2]$$

Note that the mesh size, Δx, is mesoscopic, i.e., between the microscale, $O(1\text{ km})$, and the macroscale, $O(10{,}000\text{ km})$, and that $\bar{\sigma}_I$ can have any value in the range $0 \le \bar{\sigma}_I \le 1$. Here in Eq. **2** and elsewhere in the article, discrete sums over microscopic mesh values (of order 1 km) and continuous integrals are utilized interchangeably for notational convenience.

As discussed in ref. 1, the microscopic CIN sites interact with each other and with the external mesoscopic variables, $\vec{u}_j$, through a set of plausible interaction rules. These rules are summarized through the microscopic energy for CIN in the boundary layer given by

$$H_h(\sigma_I) = \frac{1}{2}\sum_{x\neq y} J(x-y)\sigma_I(x)\sigma_I(y) + h_{\text{ext}}\sum_x \sigma_I(x), \qquad [3]$$

where J is a symmetric interaction potential and h_{ext} is an external potential. Note that the microscopic energy is a monotonic increasing function of the external field h_{ext}. The boundary layer states are regarded as a heat bath coupled to the meso-

Abbreviations: GCM, general circulation models; CIN, covective inhibition; PAC, potential for deep convection; CAPE, convectively available potential energy.

[§]To whom correspondence should be addressed. E-mail: jonjon@cims.nyu.edu

scopic variables $\vec{u}_j$ via the external potential h_{ext} such that the equilibrium statistics are given by the Gibbs measure

$$G(\sigma) = \frac{1}{Z_\Lambda} e^{\beta H_h(\sigma)} d\sigma. \quad [4]$$

For the microscopic dynamics, a configuration randomly flips at a site x,

$$\sigma_I^x(y) = \begin{cases} 1 - \sigma_I(y), \text{ if } y = x \\ \sigma_I(y) \text{ if } y \neq x \end{cases} \quad [5]$$

as a jump Markov process where the rate $c(\sigma, x)$ is given by the Arrhenius adsorption/desorption model

$$c(\sigma, x) = \begin{cases} \frac{1}{\tau_I} e^{-\beta V(x)}, \text{ if } \sigma_I(x) = 1 \\ \frac{1}{\tau_I} \text{ if } \sigma_I(x) = 0 \end{cases} \quad [6]$$

and for which $G(\sigma)$ in Eq. **4** is the invariant measure, with

$$V(x) = \sum_{z \neq x} J(x - z)\sigma_I(z) + h_{\text{ext}}. \quad [7]$$

Here τ_I is the characteristic interaction time.

The Simplest Coarse-Grained Stochastic Model for CIN

In practical parametrization, it is desirable for computational feasibility to replace the microscopic dynamics by a process on the coarse mesh that retains critical dynamical features of the interaction. Following ref. 2 the simplest local version of the systematic coarse-grained stochastic process is developed below.

Each coarse cell Δx_k, $k = 1, \ldots, m$, of the coarse-grained lattice is divided onto l microscopic cells such that $\Delta x_k \leftrightarrow (1/l)\{1, 2, \ldots, l\}$, $k = 1, \ldots, m$. In the coarse-grained procedure from ref. 2, given the coarse-grained sequence of random variables

$$\eta_t(k) = \sum_{y \in \Delta x_k} \sigma_{I,t}(y) \quad [8]$$

such that the average in Eq. **2** verifies $\bar{\sigma}_I(j\Delta x) = \eta(k)/l$, for $j = k$ in some sense, the microscopic dynamics is replaced by a birth/death Markov process defined on the variables, $\{0, 1, \ldots, l\}$, for each k such that $\eta_t(k)$ evolves according to the following probability law.

$$\begin{aligned} &\text{Prob}\{\eta_{t+\Delta t}(k) = n + 1 | \eta_t(k) = n\} = C_a(k, n)\Delta t + o(\Delta t) \\ &\text{Prob}\{\eta_{t+\Delta t}(k) = n - 1 | \eta_t(k) = n\} = C_d(k, n)\Delta t + o(\Delta t) \\ &\text{Prob}\{\eta_{t+\Delta t}(k) = n | \eta_t(k) = n\} \\ &\qquad = 1 - (C_a(k, n) + C_d(k, n))\Delta t + o(\Delta t) \\ &\text{Prob}\{\eta_{t+\Delta t}(k) \neq n, n - 1, n + 1 | \eta_t(k) = n\} = o(\Delta t). \end{aligned} \quad [9]$$

The coarse-grained adsorption/desorption rates, respectively, are given by

$$C_a(k, \eta) = \frac{1}{\tau_I}[l - \eta(k)] \qquad C_d(k, \eta) = \frac{1}{\tau_I}\eta(k) e^{-\beta \bar{V}(k)}, \quad [10]$$

where

$$\bar{V}(k) = \bar{J}(0, 0)(\eta(k) - 1) + h_{\text{ext}} \quad [11]$$

with the coarse-grained interaction potential within the coarse cell given by $\bar{J}(0, 0) = 2U_0/(l - 1)$, where U_0 is the mean strength of the potential J (2). The coarse-grained energy content for CIN is given by the coarse-grained Hamiltonian

$$\bar{H}(\eta) = \frac{U_0}{l - 1} \sum_k \eta(k)(\eta(k) - 1) + h_{\text{ext}} \sum_k \eta(k). \quad [12]$$

The canonical invariant Gibbs measure for the coarse-grained stochastic process is a product measure given by

$$G_{m,l,\beta}(\eta) = (Z_{m,l,\beta})^{-1} e^{\beta \bar{H}(\eta)} P_{m,l}(d\eta), \quad [13]$$

where $P_{m,l}(d\eta)$ is an explicit prior distribution (2). As shown in ref. 2, the coarse-grained birth/death process above satisfies detailed balance with respect to the Gibbs measure in Eq. **12** as well as a number of other attractive theoretical features. The simplest coarse-grained approximation given above assumes that the effect of the microscopic interactions on the mesoscopic scales occurs within the mesoscopic coarse-mesh scale, Δx; otherwise, systematic nonlocal couplings are needed (2). The accuracy of these approximations is tested for diverse examples from material science elsewhere (2, 4).

The practical implementation of the coarse-grained birth/death process in Eqs. **8–11** requires specification of the parameters, τ_I, U_0, q, and the external potential $h_{\text{ext}}(\vec{u}_j)$ as well as the statistical parameter β.

The Model Deterministic Convective Parametrization

A prototype mass flux parametrization with crude vertical resolution (5, 6) is utilized to illustrate the fashion in which the coarse-grained stochastic model for CIN can be coupled to a nonstochastic convective mass flux parametrization. The prognostic variables (u, θ, θ_{eb}, and θ_{em}) are the x component of the fluid velocity, u, the potential temperature in the middle troposphere, θ, and the equivalent potential temperatures, θ_{eb} and θ_{em}, measuring, respectively, the potential temperatures plus moisture content of the boundary layer and middle troposphere. The vertical structure is determined by projection on a first baroclinic heating mode (5, 6). The dynamic equations for these variables in the parametrization are given by

$$\begin{aligned} &\frac{\partial u}{\partial t} - \bar{\bar{\alpha}} \frac{\partial \theta}{\partial x} = -\left(C_D^0 \frac{1}{h}\sqrt{u_0^2 + u^2}\right)u - \frac{1}{\tau_D} u \\ &\frac{\partial \theta}{\partial t} - \bar{\alpha} \frac{\partial u}{\partial x} = \mathcal{S} + Q_R^0 - \frac{\theta}{\tau_R} \\ &h \frac{\partial \theta_{eb}}{\partial t} = -D(\theta_{eb} - \theta_{em}) + \left(C_\theta \sqrt{u_0^2 + u^2}\right)(\theta_{eb}^* - \theta_{eb}) \\ &H \frac{\partial \theta_{em}}{\partial t} = D(\theta_{eb} - \theta_{em}) + Q_R^0 - \frac{\theta_{em}}{\tau_R}, \end{aligned} \quad [14]$$

whereas the constants Q_R^0 and θ_{eb}^* are externally imposed and represent the radiative cooling at equilibrium in the upper troposphere and saturation equivalent potential temperature in the boundary layer. The constants h and H measure the depths of the boundary layer and the troposphere above the boundary layer, respectively. The typical values used here are $h = 500$ m and $H = 16$ km while $u_0 = 2$ m·s^{-1}. The explicit values for the other constants used in Eq. **14** and elsewhere in this section can be found in refs. 5 and 6.

The vertically integrated equivalent potential temperature given by

$$\langle\theta_e\rangle_z = \frac{1}{H+h}[h\theta_{eb} + H\theta_{em}] \approx \frac{h}{H}\theta_{eb} + \theta_{em}$$

satisfies the conservation equation

$$\frac{\partial\langle\theta_e\rangle_z}{\partial t} = \left(\frac{C_\theta^0}{H}\sqrt{u_0^2+u^2}\right)(\theta_{eb}^* - \theta_{eb}) + Q_R^0 - \frac{\theta_{em}}{\tau_R}. \quad [15]$$

That is, $\langle\theta_e\rangle_z$ is conserved in the absence of surface evaporative heating and tropospheric radiative cooling. The crucial quantities in the prototype mass flux parametrization are the terms $\mathcal{S}$ and D where $\mathcal{S}$ represents the middle troposphere heating due to deep convection, and D represents the downward mass flux on the boundary layer. The heating term $\mathcal{S}$ is given by

$$\mathcal{S} = M\sigma_c((\mathrm{CAPE})^+)^{1/2} \quad [16]$$

with M a fixed constant, σ_c the area fraction for deep convective mass flux, and CAPE $= \theta_{eb} - \gamma\theta$, the convectively available potential energy. The downward mass flux on the boundary layer, D, includes the environmental downdrafts, m_e, and the downward mass flux due to convection, m_-, which are nonnegative quantities so that

$$D = m_e + m_-$$

$$m_- = \frac{1-\Lambda}{\Lambda}m_c, \quad \Lambda \text{ precipitation efficiency} \quad [17]$$

$$m_c = \sigma_c((\mathrm{CAPE})^+)^{1/2},$$

and

$$m_e = -(1-\sigma_c)(w_e)^- \qquad (1-\sigma_c)w_e = -(m_c + H_m u_x). \quad [18]$$

In Eqs. **16–18**, the quantity $(X)^\pm$ denotes, respectively, the positive or negative part of the number X.

Coupling of the Stochastic CIN Model into the Parametrization

Eqs. **14–18** are regarded here as the prototype deterministic GCM parametrization when discretized in a standard fashion utilizing central differences on a coarse-mesh Δx with Δx ranging from 50 to 250 km. In the simulations below, $\Delta x = 80$ km. The coarse-grained stochastic CIN model is coupled to this basic parametrization. First, the area fraction for deep convection, σ_c, governing the upward mass flux strength, is allowed to vary on the coarse mesh and is given by

$$\sigma_c(j\Delta x) = [1 - \bar{\sigma}_I(j\Delta x)]\sigma_c^+ \text{ with } \bar{\sigma}_I \text{ is the average in Eq. } \mathbf{2}, \quad [19]$$

with σ_c^+ a threshold constant, $\sigma_c^+ = 0.002$ (5, 6). When the order parameter σ_I signifies strong CIN locally such that $\bar{\sigma}_I = 1$, the flux of deep convection is diminished to zero, whereas with PAC locally active, $\bar{\sigma}_I = 0$, this flux increases to the maximum allowed by the value σ_c^+. To complete the coupling of the stochastic CIN model into the parametrization, the coarse-mesh external potential, $h_{\mathrm{ext}}(\vec{u}_j)$, from Eqs. **11** and **12**, needs to be specified from the coarse-mesh values, $\vec{u}_j$. There is no unique choice of the external potential, but its form can be dictated by simple physical reasoning. Here, the plausible physical assumption is made that, when the convective downward mass flux, m_-, decreases, the energy for CIN decreases. Because the convective downward mass flux results from the evaporative cooling induced by precipitation falling into dry air, it constitutes a mechanism that carries negatively buoyant cool and dry air from the middle troposphere onto the boundary layer, hence tending to reduce CAPE and deep convection. Thus, the decreasing of this flux will allow the boundary layer to be able to self-consistently reduce the convective inhibition; thus, here

$$h_{\mathrm{ext}}(j\Delta x, t) = m_-(j\Delta x, t). \quad [20]$$

The other parameters needed in the birth/death process are the characteristic time τ_I, which varies over 5, 10, and 20 days below while the microscale occupation fraction $l = 10$. This is consistent with small-scale variation of CIN on the scale of 8 km. Finally, the strength of local interaction, βU_0, is systematically varied below from boundary layer interactions favoring CIN with $\beta U_0 > 0$ to those favoring PAC with $\beta U_0 < 0$. The parameter β is fixed to $\beta = 1$ such that variations in the mean interaction strength, U_0, will not directly alter the effects of the external field on the adsorption/desorption rates. This completes the specification of the coarse-grained stochastic model.

The Effects of Stochastic Parametrization on Climatology and Fluctuations

To mimic crudely the climatology of the warm pool in the Indian Ocean/Western Pacific and its associated Walker circulation, a 40,000-km domain periodic in x is utilized, and warmer humid air is prescribed in the boundary layer flux over a symmetric region of 5,000 km in extent centered at the midpoint 20,000 km. This is accomplished by raising the prescribed boundary layer saturation equivalent potential temperature, $\theta_{eb}^*(x)$, such that

$$\frac{\theta_{eb}^*(x)}{\theta_{eb}^{*,0}} = \begin{cases} 1 + A_0\cos\left(\dfrac{\pi(x-x_0)}{L_0}\right), & |x-x_0| < \dfrac{L_0}{2} \\ 1, & |x-x_0| \geq \dfrac{L_0}{2}, \end{cases} \quad [21]$$

where $x_0 = 20{,}000$ km, $L_0 = 5{,}000$ km, and $\theta_{eb}^{*,0} = 10$ K. Here A_0 is a positive constant that controls the strength of the imposed evaporative heating and below it assumes the values $A_0 = 0.5$ or $A_0 = 1$; thus, $\theta_{eb}^*(x)$ can be one and a half or twice as large as $\theta_{eb}^{*,0}$, and this maximum ratio is achieved at the center of the domain. There is no rotation in this setup, and moist gravity waves with the same structure as the moist Kelvin wave can propagate both eastward and westward (5, 6).

Below numerical results for the case of the coarse-grained birth/death stochastic process model are compared against the deterministic case of constant area fraction. Recall that from Eqs. **10** and **11**, the desorption rate, C_d, is a decreasing function of βU_0. Hence a positive value will tend to favor adsorption (C_a), by diminishing desorption, to produce CIN sites and hence giving rise to smaller statistical mean area fractions, whereas a negative value, $\beta U_0 < 0$, will favor desorption or formation of PAC sites and allows larger mean area fractions for the deep convective mass flux. Through this comparative study we will be trying to address the following fundamental issues: How does the coarse-grained stochastic parametrization of CIN affect the climatology and the wave fluctuations about this climatology compared with the deterministic parametrization? All numerical simulations reported below are started with random data and run until a statistical steady state is achieved, which takes between 50 and 100 days. The time average of this statistical steady state represents the climatology with $\bar{u}$, $\bar{q}$, and $\bar{\sigma}_c$ denoting the averaged velocity, the averaged middle troposphere water vapor mixing ratio, and the averaged area fraction. Recall that the middle tropospheric water vapor mixing ratio is given through the formula

Table 1. Effect of stochastic parameters on climatology and fluctuations with heating strength $A_0 = 0.5$

Interaction potential, βU_0	Time, τ_I, days	Climate, m·s^{-1}		Fluctuation, m·s^{-1}		Mean area fraction, $\bar{\sigma}_c$	Standard deviation, $\langle(\sigma_c - \bar{\sigma}_c)^2\rangle^{1/2}$
		$\bar{u}_-$	$\bar{u}_+$	u'_-	u'_+		
1	5	−0.856	0.855	−0.207	0.214	4.55×10^{-4}	3.00×10^{-4}
1	20	−0.855	0.856	−0.214	0.208	4.55×10^{-4}	2.96×10^{-4}
0.01	5	−1.047	1.046	−0.508	0.486	9.96×10^{-4}	3.18×10^{-4}
0.01	20	−1.048	1.040	−0.804	0.676	9.96×10^{-4}	3.15×10^{-4}
−0.01	5	−1.047	1.049	−0.603	0.572	1.00×10^{-3}	3.15×10^{-4}
−0.01	10	−0.923	0.920	−4.497	4.429	1.00×10^{-3}	3.14×10^{-4}
−0.1	5	−0.816	0.867	−4.820	4.727	1.04×10^{-3}	3.11×10^{-4}
−0.1	10	−0.824	0.877	−4.861	4.737	1.04×10^{-3}	3.12×10^{-4}

$$q = \frac{c_p}{L_v}\left(\frac{p_m}{p_0}\right)^{-.28}(\tilde{\theta}_{em} - \tilde{\theta}_m),$$

where c_p is the heat capacity of dry air, L_v is the latent heat of vaporization, p_m and p_0 are the pressures in the middle troposphere and at the ground, respectively, and $\tilde{\theta}_{em}$ and $\tilde{\theta}_m$ are the equivalent potential temperature and potential temperature in the middle troposphere augmented by a background climatological constant in order to fit, at radiative-convective equilibrium, onto a given tropical sounding (7). The fluctuations in these quantities about this climate mean are denoted by u', q', σ'_c, etc.

Quantitative information on the climatology and fluctuations for a wide range of parameters βU_0, τ_I, for $A_0 = 0.5$, 1 are presented in Tables 1 and 2. The strength of the velocity in the climatology, $\bar{u}_- \leq \bar{u} \leq \bar{u}^+$, the strength of velocity fluctuations, $u'_- \leq u' \leq u'_+$, the mean area fraction, $\bar{\sigma}_c$, and the standard deviation in the spatial fluctuations of the area fraction are reported in these tables. Obviously, increasing A_0 increases the strength of the climatology. Several other general trends in these results are apparent. First, all of the simulations have a genuinely stochastic coupling because there is always a substantial nontrivial deviation in the mean area fraction; also, the velocity magnitude in the climatology correlates strongly with this mean area fraction, which controls the heating on average, with smaller values of $\bar{\sigma}_c$ generally yielding weaker magnitudes of the climatological mean velocity except when there are very strong velocity fluctuations. As regards the fluctuations, decreasing βU_0 from the CIN statistical regime with $\beta U_0 > 0$ to the PAC statistical regime for $\beta U_0 < 0$ for a given τ_I always increases the magnitude of the wave fluctuations; also increasing the stochastic interaction time, τ_I, for a fixed βU_0 tends to increase the magnitude of the wave fluctuations. It is also interesting to compare these results with the stochastic parametrization with those obtained with the completely deterministic convective parametrization with the mean constant value, $\bar{\sigma}_c$, obtained from Table 1 to see the important differences in both climatology and fluctuations induced by the stochastic model. These are some remarkable differences discussed next for two separate cases.

Moderate Walker Forcing: $A_0 = 0.5$. In Figs. 1 and 2 the climatological mean velocity at the bottom of the troposphere given by $\bar{u}$ and the climatological middle troposphere water vapor mixing ratio are presented for three instructive examples from Table 1. In Fig. 1, the stochastic parametrization defines a strong CIN regime for $\beta U_0 = 1$ and $\tau_I = 20$ days; the full velocity structure is also displayed in Fig. 1 and has the structure of a classical Walker cell with rising air over the heating region, large-scale descent, and strong middle troposphere moisture concentration in the stronger heating region. In Fig. 2, the stochastic parameters define a weak PAC regime with $\beta U_0 = -0.01$ and $\tau_I = 5$ days represented by the solid curves. This climatology is a slightly stronger Walker cell, and the mean area fraction is significantly larger. From Table 1 the velocity fluctuations are ≈20% for the case in Fig. 1 but rise to 40–60% for the case with $\tau_I = 5$ days in Fig. 2. The dashed curves in Fig. 2 demonstrate that the climatology bifurcates to a completely different character that is no longer an elementary Walker cell by keeping the value of $\beta U_0 = -0.01$ but increasing the stochastic interaction time to $\tau_I = 10$ days. In fact, the fluctuations are >400% of the mean state, and Fig. 3 demonstrates that in fact the actual dynamical solution is a time-periodic state consisting of two moist gravity waves propagating symmetrically eastward and westward from the heating region. This structure persists for all smaller βU_0 and all τ_I in Table 1. On the other hand, the climatology with the deterministic parametrization for area fractions given by, $\bar{\sigma}_c = 0.0005, 0.001$ from Table 1 is a radically different climatology than any of the results in Figs. 1–3 and never is a classical Walker cell; in both of these deterministic cases, the mean climatology resembles somewhat the one represented by the dashed curves in Fig. 2 but with weaker amplitudes and a nonzero (spatial) mean wind such that the fluctuations consist of an individual giant moist gravity wave propagating in one direction against the weak mean flow through the wind-

Table 2. Effect of stochastic parameters on climatology and fluctuations with heating strength $A_0 = 1$

Interaction potential, βU_0	Time, τ_I, days	Climate, m·s^{-1}		Fluctuation, m·s^{-1}		Mean area fraction, $\bar{\sigma}_c$	Standard deviation, $\langle(\sigma_c - \bar{\sigma}_c)^2\rangle^{1/2}$
		$\bar{u}_-$	$\bar{u}_+$	u'_-	u'_+		
1	5	−1.417	1.417	−0.536	0.436	4.56×10^{-4}	3.00×10^{-4}
1	20	−1.415	1.417	−0.330	0.546	4.56×10^{-4}	3.00×10^{-4}
0.01	5	−1.692	1.691	−1.196	1.603	9.96×10^{-4}	3.17×10^{-4}
0.01	20	−1.692	1.691	−1.180	1.266	9.96×10^{-4}	3.17×10^{-4}
−0.01	5	−1.693	1.693	−1.421	1.470	1.00×10^{-3}	3.15×10^{-4}
−0.01	10	−1.693	1.693	−1.277	1.243	1.00×10^{-3}	3.16×10^{-4}
−0.1	5	−1.700	1.699	−0.990	1.092	1.04×10^{-3}	3.10×10^{-4}
−0.1	10	−1.700	1.700	−1.447	1.269	1.04×10^{-3}	3.07×10^{-4}

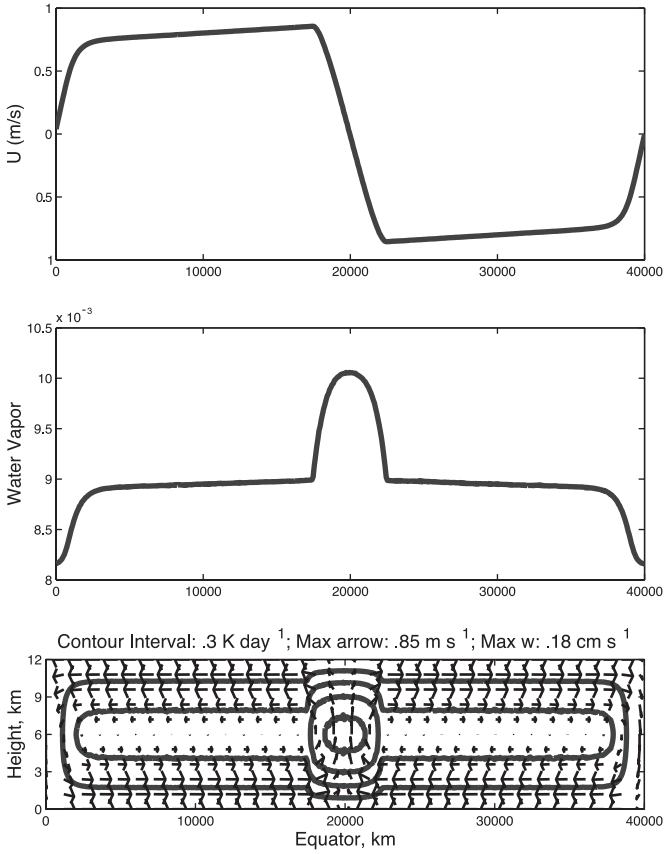

Fig. 1. Walker cell in the strong CIN regime: $\beta U_0 = 1$, $\tau_l = 20$ days, and $A_0 = 0.5$. (*Top*) Mean zonal velocity at the bottom of the troposphere. (*Middle*) Mean middle tropospheric water vapor mixing ratio. (*Bottom*) Vertical zonal structure of the mean flow and contours of the mean convective heating. Vertical velocity is multiplied by a factor of 60 to account for the aspect ratio.

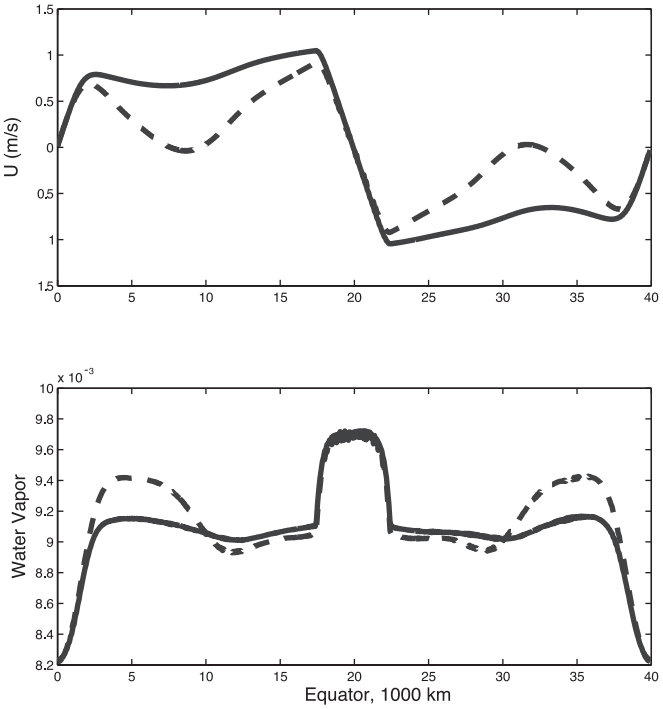

Fig. 2. Mean zonal velocity at the bottom of the troposphere (*Upper*) and mean middle tropospheric water vapor content (*Lower*) for the parameters $\beta U_0 = -0.01$, $A_0 = 0.5$, with $\tau_l = 5$ days (solid line) and $\tau_l = 10$ days (dashed line).

induced surface heat exchange instability (5). This is unlike Fig. 3 (symmetry breaking) where we have two distinct waves of comparable magnitude propagating in opposite directions and compensating each other at the center and at the extremities of the domain.

Strong Walker Forcing: $A_0 = 1$. As shown in Table 2, increasing the heating strength to $A_0 = 1$ always yields a basic stable Walker cell in the climatology for the stochastic parametrization with increasing wave fluctuations as βU_0 decreases. The strength and nature of the wave fluctuations structures for $\beta U_0 = 0.01$ are $\approx 60\%$ and no longer depends sensitively on τ_l in that regime. In this case with $A_0 = 1$, the deterministic parametrization with the appropriate mean area fraction from Table 2 always gave essentially the same Walker cell as the climatological mean state for the stochastic parametrization; however, for the deterministic case, this Walker cell is a genuine nonlinear steady state, and the wave fluctuations are completely absent, unlike the stochastic cases that have strong wave fluctuations.

Concluding Discussion

Prototype coarse-grained stochastic parametrizations for the interaction with unresolved features of tropical convection have been introduced and developed here. These stochastic parametrizations have low computational overhead and allow the systematic coupling of the coarse-grained variables to the stochastic process through the interaction potential, $h_{\text{ext}}(\vec{u}_j)$, with other key parameters, βU_0, the coarse-grained microscopic interaction potential for the boundary layer dynamics, and τ_l, the interaction time for the stochastic feedback on the dynamics. It was established here that these features in suitable regimes can both drastically alter the climatology and increase the wave

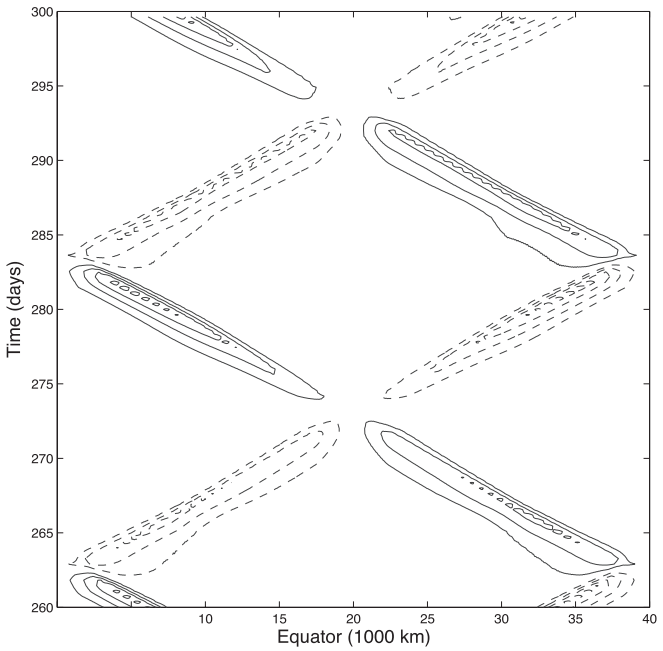

Fig. 3. Contours of the fluctuations in zonal velocity, u, in the x–t plan displaying the formation of giant waves after the bifurcation in Fig. 2 occurs, i.e., $\beta U_0 = -0.01$, $A_0 = 0.5$, and $\tau_l = 10$ days. Positive, solid line; negative, dashed line; contour interval, 1 m·s^{-1}.

fluctuations compared with standard deterministic parametrizations. In another new direction, Lin and Neelin (8, 9) recently developed another interesting class of stochastic parametrizations with more passive input of the large scales on the small-scale processes represented as stochastic noise. The coarse-grained stochastic models introduced here are only the simplest ones in a hierarchy that allows for nonlinear interaction (2, 4) and should also be compared and tested with detailed microscopic models for a wide range of parameters as well as the alternative stochastic strategies (8, 9).

A.J.M. is partially supported by National Science Foundation Grant NSF-DMS-9972865, Office of Naval Research Grant ONR-N00014-96-1-0043, and Army Research Office Grant ARO-DAADI9-01-10810. B.K. was supported as a postdoctorate on these grants. M.A.K. is partially supported by National Science Foundation Grants NSF-DMS-0100872 and NSF-ITR-0219211.

1. Majda, A. J. & Khouider, B. (2002) *Proc. Natl. Acad. Sci. USA* **99,** 1123–1128.
2. Katsoulakis, M. A., Majda, A. J. & Vlachos, G. D. (2003) *Proc. Natl. Acad. Sci. USA* **100,** 782–787.
3. Mapes, B. (2000) *J. Atmos. Sci.* **57,** 1515–1535.
4. Katsoulakis, M. A., Majda, A. J. & Vlachos, G. D. (2003) *J. Comput. Phys.* **186,** 250–278.
5. Majda, A. J. & Shefter, M. (2001) *J. Atmos. Sci.* **58,** 896–914.
6. Majda, A. J., Khouider, B., Kiladis, G. N., Straub, K. & Shefter, M. (2003) *J. Atmos. Sci.*, in press.
7. Gill, A. E. (1982) *Atmosphere-Ocean Dynamics* (Academic, San Diego).
8. Lin, J. W.-B. & Neelin, D. (2000) *Geophy. Res. Lett.* **27,** 3691–3694.
9. Lin, J. W.-B. & Neelin, D. (2003) *Geophys. Res. Lett.* **30,** 1162–1165.